

Electronic Supplementary Information

Boron “gluing” nitrogen heteroatoms in prepolymerized ionic liquid-based carbon scaffold for durable supercapacitive activity

Ling Miao ^a, Hui Duan ^a, Dazhang Zhu ^a, Yaokang Lv ^c, Lihua Gan ^a, Liangchun Li ^{a, *}, Mingxian Liu ^{a, b, *}

^aShanghai Key Lab of Chemical Assessment and Sustainability, School of Chemical Science and Engineering, Tongji University, Shanghai 200092, P. R. China.

^bCollege of Chemistry and Molecular Engineering, Zhengzhou University, Zhengzhou 450001, P. R. China.

^cCollege of Chemical Engineering, Zhejiang University of Technology, Hangzhou 310014, P. R. China.

*Corresponding Authors

E-mail: lilc@tongji.edu.cn (L. Li), liumx@tongji.edu.cn (M. Liu).

Fig. S1. ¹H NMR spectrum of the typical monomeric ionic liquid (a). CNMR spectrum of *p*[ABA-*co*-MA][PA]-2:1 (b). FT-IR spectra of *p*[MA][PA], *p*[ABA-*co*-MA][PA]s, *p*[ABA][PA] (c). TGA curves of *p*[ABA-*co*-MA][PA]-2:1 and RbOH@*p*[ABA-*co*-MA][PA]-2:1 (d, inset is the DSC curve of RbOH@*p*[ABA-*co*-MA][PA]-2:1).

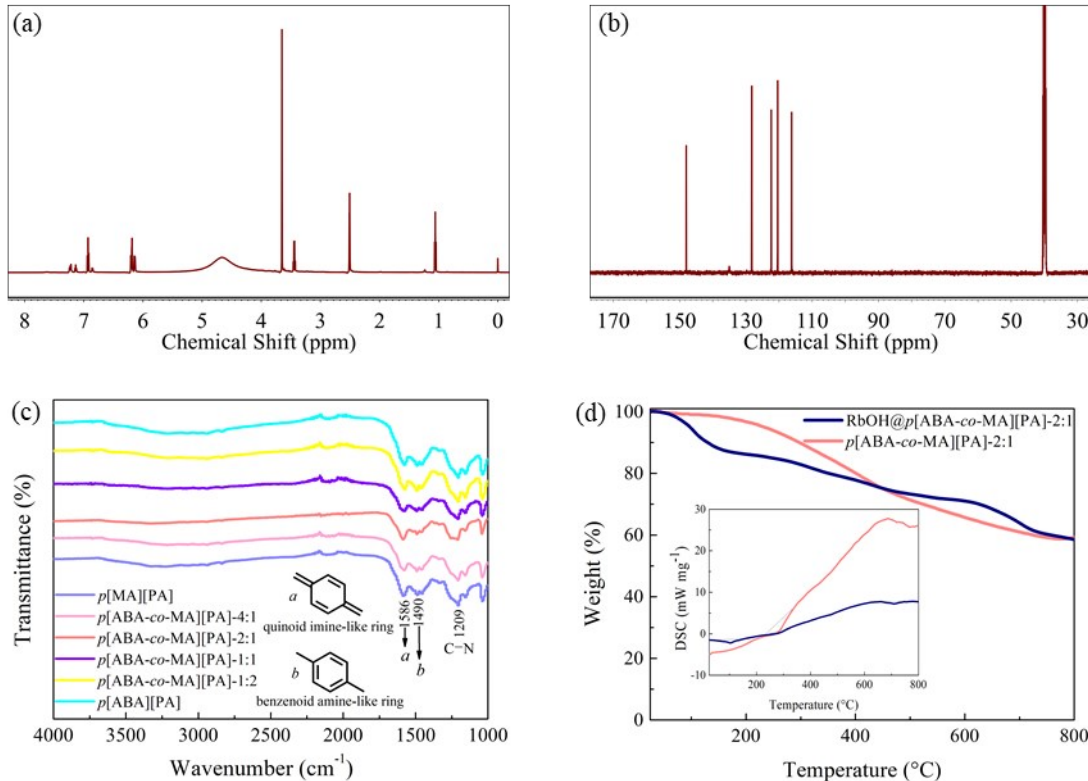


Fig. S2. SEM images of CPIL-2 (a), CPIL-4 (b), CPIL-6 (c).

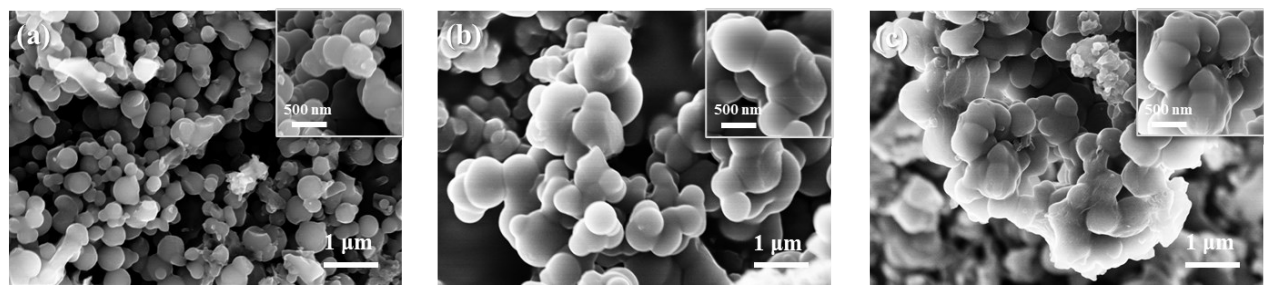


Fig. S3. XRD patterns (a) of CPILs. High resolution TEM image of CPIL-3 (b, inset is the selected area electron diffraction pattern). Raman spectra (c) and electronic conductivities (d) of CPILs.

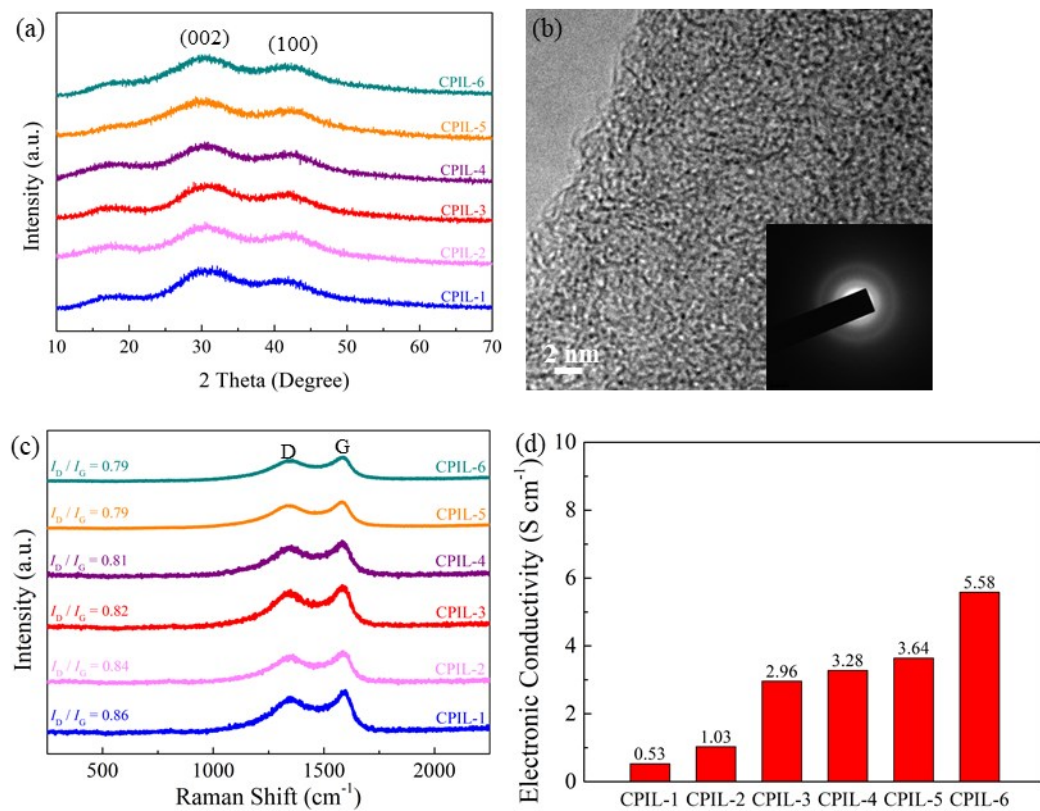


Fig. S4. Electrochemical properties of CPIL-3 in a H₂SO₄-based three-electrode configuration: CV curves (a), absolute current density and sweep rate follow the power law $i=kv^b$ in the charging/discharging processes (b), the relationship between the sweep rate and capacitive contribution (c). Electrochemical properties of CPIL-1 and CPIL-2 in a H₂SO₄-based three-electrode configuration: CV curves (d, g), decoupling capacitive contributions at 5 mV s⁻¹ (e, h), the relationship between the sweep rate and capacitive contribution (f, i).

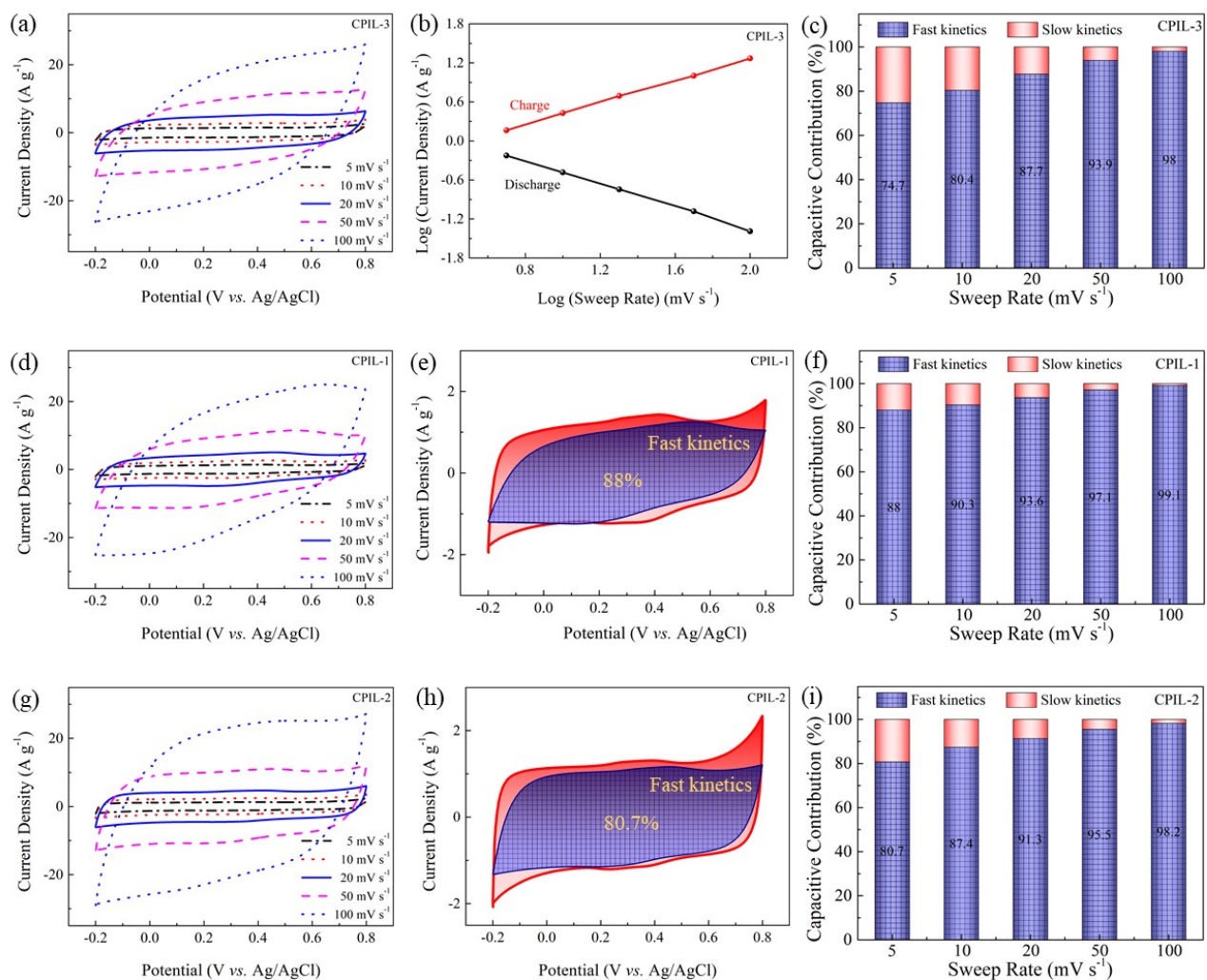


Fig. S5. Electrochemical properties of CPIL-4, CPIL-5 and CPIL-6 in a H₂SO₄-based three-electrode configuration: CV curves (a, d, g), decoupling capacitive contributions at 5 mV s⁻¹ (b, e, h), the relationship between the sweep rate and capacitive contribution (c, f, i).

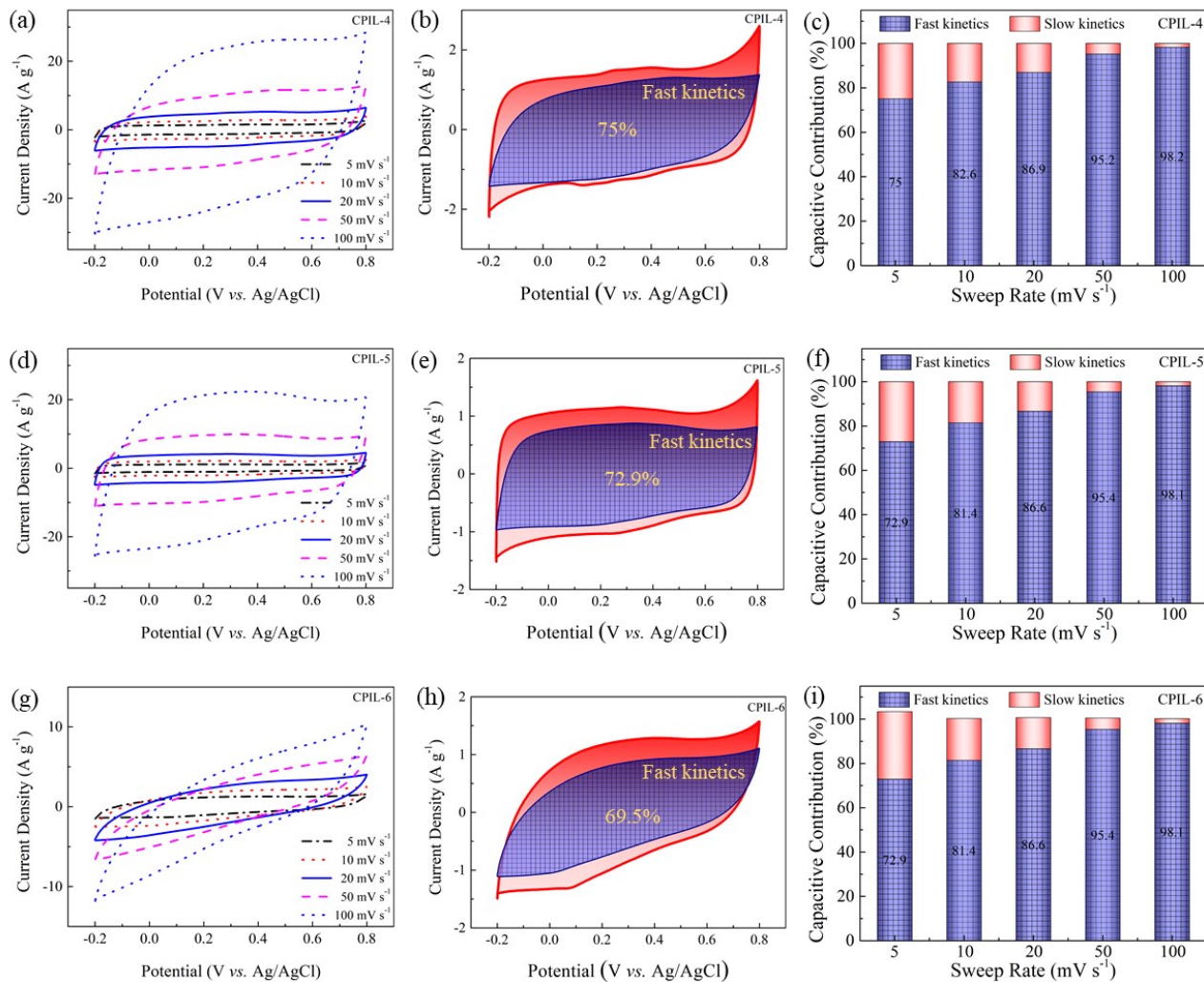


Fig. S6. Electrochemical properties in a H_2SO_4 -based three-electrode configuration: GCD curves

(a–f), the relationship between capacitance and current density (g). Electrochemical properties in a H_2SO_4 -based two-electrode cell: GCD curves of CPIL-3-loaded device @ 10 A g^{-1} before and after 100000 cyclic turns (h).

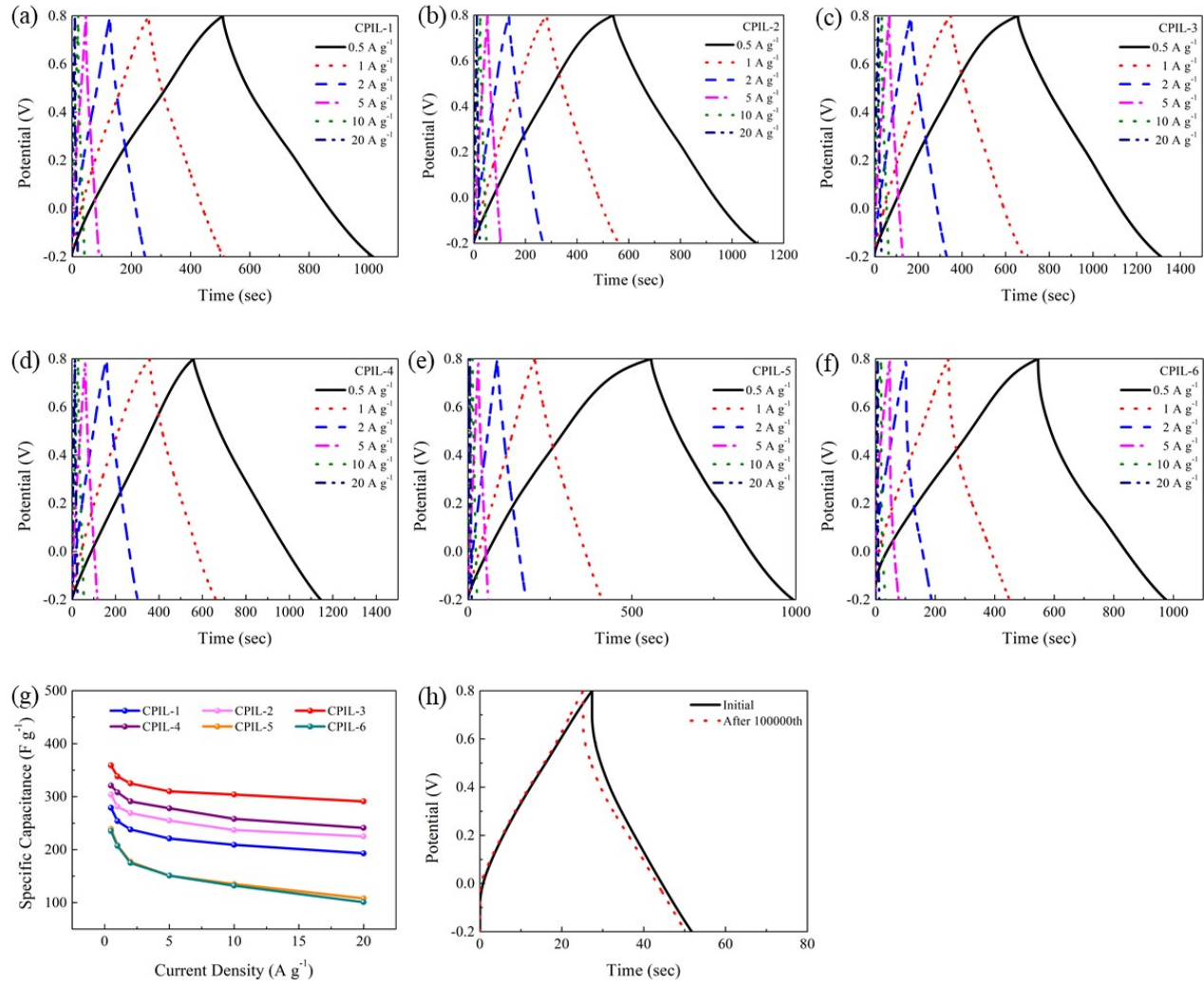


Fig. S7. GCD curves tested in the TMA-BF₄/EMIM-BF₄-based two-electrode cells.

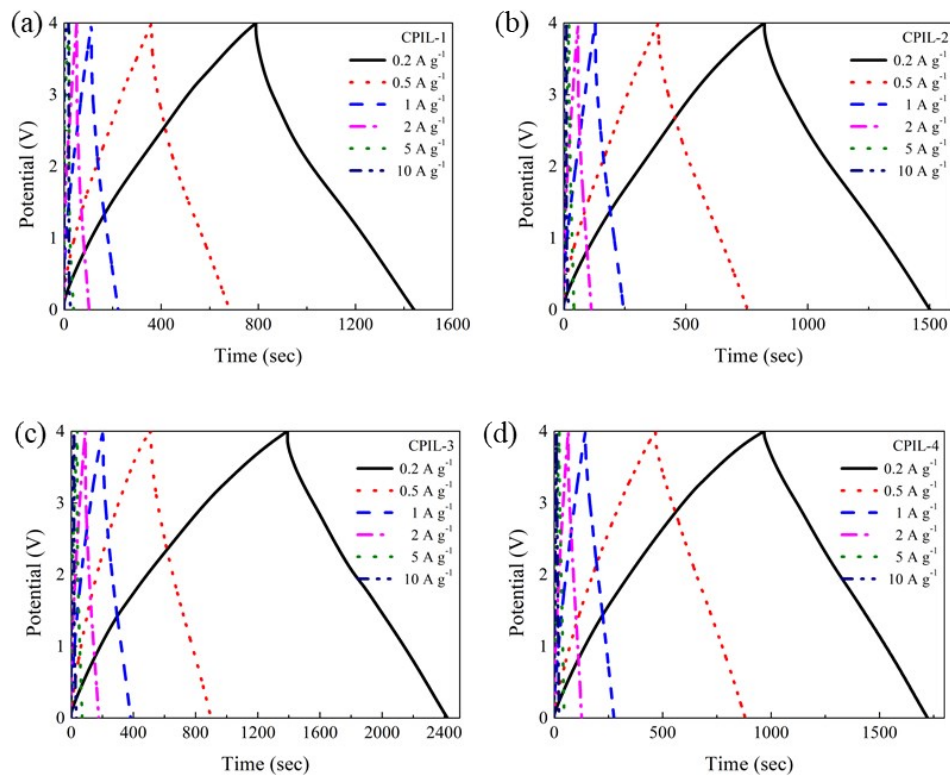


Table S1. The capacitance comparison of various heteroatoms-doped porous carbons.

Samples	S_{BET} ($\text{m}^2 \text{ g}^{-1}$)	Heteroatom content (at.%)	Electrolyte	Capcitance (F g^{-1})	Ref.
CPIL-3	2629	N/B/O: 7.55/6.38/9.20	H_2SO_4	359 (0.5 A g^{-1})	This work
			TMA-BF ₄ /EMIM-BF ₄	209 (0.2 A g^{-1})	
p-TIDN@600	1374.19	N/O: 7.58/5.32	H_2SO_4	231.35 (0.1 A g^{-1})	1
NPOC-900-0.5	1177	N/P/O: 4.29/1.94/7.26	H_2SO_4	215 (1 mV s^{-1})	2
NCFN2-900	391	N/O: 7.03/6.25	H_2SO_4	211 (1 A g^{-1})	3
NPCN	394	N/P: 6.9/0.68	H_2SO_4	267 (1 A g^{-1})	4
N-HMCS/S	1230	N/O: 1.7/3.2 (wt.%)	KOH	196.5 (0.5 A g^{-1})	5
PCN-6	1907	N/O: 1.54/6.59	KOH	280 (0.5 A g^{-1})	6
C-0.75-900	2872.2	N/O: 2.24/2.44	EMIM-BF ₄	175 (0.5 A g^{-1})	7
DCNF	870	–	EMIM-BF ₄	133 (1 A g^{-1})	8
STC-16	2324	N: 5.43 wt.%	EMIM-BF ₄	178 (0.2 A g^{-1})	9
NCAC	1510	–	BMPYTFSI	84 (0.1 A g^{-1})	10
LAC800:4	2038	–	BMIM-BF ₄	175 (0.5 A g^{-1})	11
HHCF	2766	N/O: 0.41/6.95	EMIM-BF ₄	174 (1 A g^{-1})	12
OMCNS	442	O: 8.1	EMIM-BF ₄	130 (0.5 A g^{-1})	13

References

- 1 F. Y. Hu, T. P. Zhang, J. Y. Wang, S. M. Li, C. Liu, C. Song, W. L. Shao, S. Y. Liu and X. G. Jian, *Nano Energy*, 2020, **74**, 104789.
- 2 C. Cui, Y. Gao, J. Li, C. Yang, M. Liu, H. Jin, Z. Xia, L. Dai, Y. Lei, J. Wang and S. Wang, *Angew. Chem. Int. Ed.*, 2020, **59**, 2–8.
- 3 H. Chen, T. Liu, J. Mou, W. Zhang, Z. Jiang, J. Liu, J. Huang and M. Liu, *Nano Energy*, 2019, **63**, 103836.
- 4 V. S. Kale, M. Hwang, H. Chang, J. Kang, S. I. Chae, Y. Jeon, J. Yang, J. Kim, Y.-J. Ko, Y. Piao and T. Hyeon, *Adv. Funct. Mater.*, 2018, **28**, 1803786.
- 5 J. Du, L. Liu, Y. Yu, Z. Hu, B. Liu and A. Chen, *ACS Appl. Mater. Interfaces*, 2018, **10**, 40062–40069.
- 6 J. Yu, C. Yu, W. Guo, Z. Wang, S. Li, J. Chang, X. Tan, Y. Ding, M. Zhang and L. Yang, *Nano Energy*, 2019, **64**, 103921.
- 7 J. Li, N. Wang, J. Tian, W. Qian and W. Chu, *Adv. Funct. Mater.*, 2018, **28**, 1806153.
- 8 J. Wang, J. Tang, Y. Xu, B. Ding, Z. Chang, Y. Wang, X. Hao, H. Dou, J. H. Kim, X. Zhang and Y. Yamauchi, *Nano Energy*, 2016, **28**, 232–240.
- 9 R. Yan, M. Antonietti and M. Oschatz, *Adv. Energy Mater.*, 2018, **8**, 1800026.
- 10 Z. Li, J. Liu, K. Jiang and T. Thundat, *Nano Energy*, 2016, **25**, 161–169.
- 11 W. Sangchoom, D. A. Walsh and R. Mokaya, *J. Mater. Chem. A*, 2018, **6**, 18701–18711.
- 12 X. Deng, J. Li, S. Zhu, L. Ma and N. Zhao, *Energy Storage Mater.*, 2019, **23**, 491–498.
- 13 J. Wang, Y. Xu, B. Ding, Z. Chang, X. Zhang, Y. Yamauchi and K. C.-W. Wu, *Angew. Chem. Int. Ed.*, 2018, **57**, 2894–2898.